

## **SURFACE INTEGRITY EXAMINATION OF MACHINED SPECIMENS BY USING ATOMIC FORCE MICROSCOPY**

Hulas R. TONDAY<sup>1</sup>, Pravin K. SINGH<sup>2</sup>

*Inconel 718 is a used as a work material, which is a precipitation-hardened alloy possessing oxidation and corrosion resistance having wide range of applications. The primary aim of this work is to assess the surface integrity of machined specimens by making use of atomic force microscopy. The secondary aim is to accomplish statistical analysis of surface roughness based on different set of machining parameters. In the current research, Taguchi's  $L_{16}$  orthogonal arrays are adopted and sixteen numbers of Inconel 718 samples have been produced by utilizing the wire EDM. A significant illustration has also been presented by probing the surface topographies, cross-section profiles, and roughness graphs to confirm the influence of machining variables on surface integrity. The cutting voltage is detected as the most significant machining variable when estimated by ANOVA.*

**Keywords:** Atomic force microscopy; Wire EDM; Surface parameters; Surface topography; Inconel 718; Taguchi method.

### **1. Introduction**

In this research, a relationship has been developed in the three major fields namely surface characteristics, atomic force microscopy (AFM), and wire electrical discharge machining of Inconel 718. Furthermore, wire electrical discharge machining (wire EDM) process is chosen to prepare the samples of micro-sizes; AFM technique has been selected for probing sample surfaces for obtaining and understanding the surface characteristics. However, published research works in these three fields have been reviewed critically. The surface topography is a significant feature of a component that affects the mechanical and physical characteristics as well as coatings and optical features. Surface topography also plays an essential role in the functioning of a product while utilizing in incompatible zones such as friction, lubrication, sealing, wear, bearing surfaces and optics.

---

<sup>1</sup>Department of Mechanical Engineering, Shreeyash College of Engineering & Technology, Aurangabad, MH- 431005, INDIA, e-mail: hulasniff13@gmail.com

<sup>2</sup>Department of Mechanical Engineering, Amity University Jharkhand, INDIA, e-mail: pravinsingh.phd@gmail.com

Consequently, the metrology and evaluation of surface topography inveigled the researchers from both educational institutes and industries [1]. The metrology of surface topography has been brought forward as two major regions such as precision metrology and 3D assessment. Even the high precision characterization of 2-D profiles imparts inadequate information about the actual topography of the sample surface, whereas the 3D non-parametric assessment of a sample could deliver an overall illustration of the surface topography [2]. As the AFM has been utilized for the assessment of machined surfaces in the present research work, relevant literatures from this field have been studied and delineated as a further matter. The AFM is a kind of scanning probe microscopy which results in precise and accurate three-dimensional images for examining surface topography and morphology in quantitative as well as qualitative terms. As the AFM has been utilized for the assessment of machined surfaces in the present research work, relevant literature from this field have been studied and delineated as a further matter. The AFM is a kind of scanning probe microscopy that results in precise and accurate three-dimensional images for examining surface topography and morphology in quantitative as well as qualitative terms. The significant merit of AFM is that it can analyze solid conductive materials as well as non-conductive materials such as biological cells or molecules and powder materials which are not possible by scanning tunneling microscopy (STM) [3, 4]. Average roughness, surface skewness, root mean squares, the maximum height, and kurtosis are significant surface parameters for analysis of surface topography as quantitative data and vertical amplitude. It is necessary to evaluate these parameters and surface micrographs to obtain significant information about surface properties of Inconel 718 material [5, 6]. Kojic et al. [7] developed a correlation between surface topography and nanomagnetic features of lead telluride alloy by using the AFM technique. They figured out the size of nanomagnetic particles and evaluated the diamagnetic and paramagnetic domains. Thakur et al. [8] examined the influence of machining feed and tool coatings on machined surface roughness and machinability of Inconel 825 and demonstrated that coated tool produced a desirable surface finish. Tonday and Tigga [9] also utilized the AFM technique to characterize the surface topography of Ti6Al4V Samples and observed those surface parameters are dependent on the machining factors. Lin and Hsu [10] employed the AFM probe to form nano-grooves on the sapphire surface and analyzed the input parameters and their influence on experimental results.

In the current research, different samples have been produced by using various combinations of machining parameters of wire EDM. Therefore, it is essential to study the literature related to the fields of wire EDM and its operational analysis. Wire EDM a material removal technique in which a potential difference is allowed between a thin wire and workpiece electrodes, in the

presence of dielectric fluid, due to which electrical discharges have been generated consecutively. The electrically conductive workpiece is cut out due to the melting and evaporation of tiny particles from the workpiece as well as the wire electrode [11]. Uneven and abnormal surface defects caused fractures, adhesion of impurities and gloss; and these defects limit wide applications of Inconel 718 materials in precision, tool, and medical engineering industries. Part of Inconel 718 material machined by conventional techniques results in abnormal surfaces with metal strips, scratches and pits and tool marks [12]. These parts require additional extensive and expensive surface treatments and coatings that increase the cost of machining such parts. To avoid these problems non-traditional machining process such as wire EDM has been used for machining such parts of hard materials in complex profiles and shapes [13].

Substantial research works have been performed in the field of wire EDM process in which its mechanism of machining, machinability have been evaluated such as Kanlayasiri and Boonmung [14] came upon that pulse on time and pulse peak current had been important factors affecting the surface roughness during machining of DC53 die steel. Spedding & Wang [15] formulated the response surface methodology and artificial neural network models for predicting the output parameters such as cutting speed, surface waviness, and surface roughness in machining of AISI 420 material by wire EDM. But they have not described the effects of wire EDM parameters on surface characteristics comprehensively using advanced measuring and imaging methods. Fedorov et al. [16] assessed the causes of wire breakage during the wire-EDM process in the cutting of steel 36CrNiMo4. The wire breakages have been categorized as explicit and implicit breakages. They mainly elaborated on the Rehbinder effect and its influence on the wire damage at the time of machining operations. Takale and Chougule [17] utilized an optimized wire EDM process for producing a highly accurate and great biocompatible orthopedic implant of TiNi alloy. The major interest is about surface characteristics of the machined component. They have looked over the response parameters of machining. A wide range of published literature has been studied for overview and exploration of the entire and recent circumferences of knowledge in the above-mentioned areas. Thus, a research gap has been presented in the next paragraph.

A little research has been found in which the Inconel 718 surface has been analyzed by the AFM method. None of a published article is found in which the surface machined by wire EDM process has been examined using AFM and measured the surface topography. The aim of the current work is to characterize the surface topography, textures, and morphologies of the different samples, which are produced by the wire EDM process, using the AFM technique. The effects of sample processing techniques on surface textures have also been examined and compared to the results obtained. A relationship between opted

cutting parameters and surface roughness has been formulated and modeled using Taguchi's linear model analysis and analysis of variance (ANOVA).

## 2. Materials and Methods

A commercially available and cold rolled Inconel 718, a superalloy has been used as a sample material in a rectangular shape. It is the most widely used and well-established superalloy with great mechanical properties. It has broad applications and scope in aerospace, automobile, marine, nuclear plants, and medical industries [13]. The workpieces have been machined and the desired shape and size are acquired by using Fanuc ROBOCUT  $\alpha$ -OiC CNC Wire cut EDM machine tool. During this experimental work, the selection of machining variables and their levels is based on the literature reviewed and specification of the machine tool used [17, 18]. The cutting parameters such as pulse on time, cutting voltage, pulse off time, and wire tension have been considered for experimental design and each of them possesses values in two different levels, whereas the remaining cutting variables viz. pulse current (1.5 Amperes), wire feed (14 m/minute), flushing pressure ( $1.37 \times 10^6$  MP<sub>a</sub>), and servo voltage (70 Volts) etc. contains fixed values. Table (1) shows the cutting variables of wire EDM process and corresponding levels. The size of the specimen preferred for investigation on the wire EDM and AFM is in rectangular shapes of  $9 \times 9$  mm<sup>2</sup> area and 0.3 millimeter thickness.

Table 1

Cutting parameters of wire EDM process and corresponding levels

| Number | Parameters      | Units      | Levels |      |
|--------|-----------------|------------|--------|------|
|        |                 |            | I      | II   |
| 1      | On Time         | Ms         | 5      | 8    |
| 2      | Off Time        | Ms         | 30     | 42   |
| 3      | Wire Tension    | Gram-force | 1320   | 1370 |
| 4      | Cutting Voltage | V          | 26     | 30   |

An AFM make of NT-MDT, SOLVER PRO, SPM, Russia, has been employed for surface characterization of Inconel 718 samples. Measurements of surface parameters have been done in nano and micro scales using the scan size of  $5 \times 5$   $\mu\text{m}^2$  per scan of the samples' surfaces in contact mode operation under ambient conditions. In AFM, a conductive probe with small Titanium Nitride tip moves on the specimen surface. The probe, having a radius of 18 nm, is fastened with an adjustable silicon cantilever [5]. Due to the sensor of forces and specimen contact with the probe, details of surface properties are recorded in terms of three-dimensional images, graphs, quantitative data, and qualitative facts. The recorded surface images have been analyzed by NOVA 1.0.26 Rc1 software. NOVA is the

authentic software program that provides a technique for nano and microscale image processing and for exporting quantitative information of surface properties.

### 3. Results and Discussion

In this research, wire EDM is taken into consideration because it is a non-contact type of machining process, i.e. there is no contact between tool and workpiece, which does not damage the machined surfaces. It is capable of machining any electrically conductive metals inattentive of its hardness, size, and complexity with adequate surface finish and topography. In the wire EDM process, sample surface texture is directly influenced by discharge energy which depends on process parameters [11]. The large craters have been formed on the sample surface due to melting and erosion generated by high input discharge energy compared to those with low discharge energy. These formations of crater diminish the surface quality and influence the precision, accuracy, and performance. Therefore, it is necessary to ascertain an optimum combination of input parameters to obtain the desired surface quality of the machined specimen of Inconel 718 [13, 17]. In this study, Taguchi's L16 orthogonal arrays have been adapted for robust factor design and experimental run have been accomplished. The workpiece cutting has been executed using each combination of parameter design. Surface roughness measured by the stylus method (surface tester) is quantified as  $R_a$  and measured in  $\mu\text{m}$ , whereas the average roughness measured by the AFM technique is measured in nanometer (nm). After each cutting, the surface roughness of the sample has been measured using the surface tester and the obtained results are shown in the table (2). It has been found from the table (2) that the sample-7 has the lowest  $R_a$  value ( $2.6 \mu\text{m}$ ) whereas the sample-14 has the highest  $R_a$  value ( $3.8 \mu\text{m}$ ) among all the sixteen samples. Taguchi's linear model analysis is used for modeling the relationship between cutting variables and the output response ( $R_a$ ). Hence, the Taguchi method assists in studying the effects of independent process parameters on the response variable.

For determining the adequacy of the formulated model, ANOVA has been taken up using observed results of surface roughness. ANOVA for means of  $R_a$  has been shown in the table (3) in which the p-values have been evaluated for 95% confidence level. A machining factor will be said to the significant factor if the corresponding p-value is less than 0.05. Similarly, machining factor will be said to the non-significant factor, if the corresponding p-value is greater than 0.05 [14, 15]. In this statistical analysis, the cutting voltage is the most significant machining parameter since the corresponding p-value is less than 0.05 which is also true in theoretical concept of wire EDM process. The main effects plot for means of  $R_a$  has been illustrated in figure (1) which shows that the cutting voltage is the most crucial machining factor influences the  $R_a$  [18].

Table 2

**Design of experiments using Taguchi's L<sub>16</sub> orthogonal arrays and experimental responses**

| Experiment Number | On Time | Off Time | Wire Tension | Cutting Voltage | R <sub>a</sub> (μm) |
|-------------------|---------|----------|--------------|-----------------|---------------------|
| 1                 | 5       | 30       | 1320         | 26              | 2.9                 |
| 2                 | 5       | 30       | 1320         | 30              | 3.66                |
| 3                 | 5       | 30       | 1370         | 26              | 2.7                 |
| 4                 | 5       | 30       | 1370         | 30              | 3.08                |
| 5                 | 5       | 42       | 1320         | 26              | 2.96                |
| 6                 | 5       | 42       | 1320         | 30              | 3.6                 |
| 7                 | 5       | 42       | 1370         | 26              | 2.6                 |
| 8                 | 5       | 42       | 1370         | 30              | 3.55                |
| 9                 | 8       | 30       | 1320         | 26              | 2.95                |
| 10                | 8       | 30       | 1320         | 30              | 3.62                |
| 11                | 8       | 30       | 1370         | 26              | 2.68                |
| 12                | 8       | 30       | 1370         | 30              | 3.47                |
| 13                | 8       | 42       | 1320         | 26              | 2.93                |
| 14                | 8       | 42       | 1320         | 30              | 3.8                 |
| 15                | 8       | 42       | 1370         | 26              | 2.8                 |
| 16                | 8       | 42       | 1370         | 30              | 3.46                |

Table 3

**ANOVA results for means of surface roughness (R<sub>a</sub>)**

| Source          | DF | SS    | MS    | F-Value | P-Value |
|-----------------|----|-------|-------|---------|---------|
| On Time         | 1  | 0.027 | 0.027 | 2.330   | 0.155   |
| Off Time        | 1  | 0.026 | 0.026 | 2.190   | 0.167   |
| Wire Tension    | 1  | 0.270 | 0.270 | 23.130  | 0.002   |
| Cutting Voltage | 1  | 2.045 | 2.045 | 174.950 | 0.000   |
| Residual error  | 11 | 0.129 | 0.129 |         |         |
| Total           | 15 | 2.497 |       |         |         |

Metrology and assessment of surface topography have been extremely significant for several advanced machining and forming processes. A producer of a component can primordially modify and amend the capabilities and area of applications of a component when the areal surface features are under control. The surface topography has the broad influence on the areas such as fluidics, tribology, biology, aerodynamics, and optics etc. and hence the suitable measurement plan and procedure are required [2]. The AFM has been applied to evaluate the surface textures produced by wire EDM process to demonstrate and justify the surface topography and morphology of the samples. The surface textures and profiles recorded from AFM technique contain distinct data set

including noises. To furnish desired data points and features of the surface, data processing has been performed by applying the commercial software NOVA; through which the noises and errors occurred during measurement and production processes, have been removed. Since the sample-7 has the lowest  $R_a$  value ( $2.6 \mu\text{m}$ ) and the sample-14 has the highest  $R_a$  value ( $3.8 \mu\text{m}$ ), both the samples have been considered for comparison and topographic investigation using AFM as the representation and comparison of all the sixteen samples are not possible in a single article due to the large number of AFM images, data set and graphs per sample. The detailed discussions of sample characterization have been construed in further subsections.

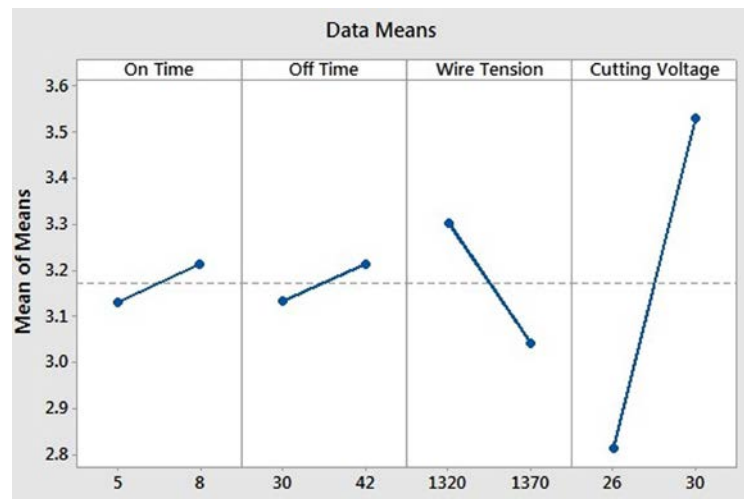


Fig. 1. Main effects plot for means of surface roughness ( $R_a$ ).

### 3.1. Discussion of characterization of sample-7

Figs. 2 (a, b) shows the 2-D micrographs and 3D topography obtained by AFM technique. In these figures, surface height features, ridges, and mounds on sample have been clearly illustrated. After analysis by NOVA software, cross section profiles along the horizontal line, vertical line, and slant line have been shown in figures 3 (a, b & c) respectively. It has been seen from these figures, how the section profiles changed in different directions of the sample surface. By data and image processing, values of surface parameters such as maximum height, ten point height, average roughness, skewness, second moment and kurtosis have been acquired as shown in the table (4). Fig. (4) shows the surface roughness profile of sample-7 in nanometer range which delineated the roughness pattern obtained by AFM which looks like Gaussian roughness graph [6, 7]. Figure (5) illustrated the threshold mask detailing the threshold at 7270 nm and the numbers of grains are 73 at the scanned area of the surface of the sample-7. Finally, 2D

Fast Fourier Transform (FFT) images of the sample have been generated in which FFT scaling is logarithmic as shown in figure 6 (a, b) respectively, which are the filtered images of AFM topography. The FFT images illustrate the relationship between eigenvectors and frequency produced by the cantilever of AFM set up. The white lines (in the middle) shown in the middle of the images is the baseline of means of noises. Since the eigenvectors are within 200, it can be said that the retrieved responses through AFM analysis are highly conspicuous and apparent to describe the topography of the machined sample.

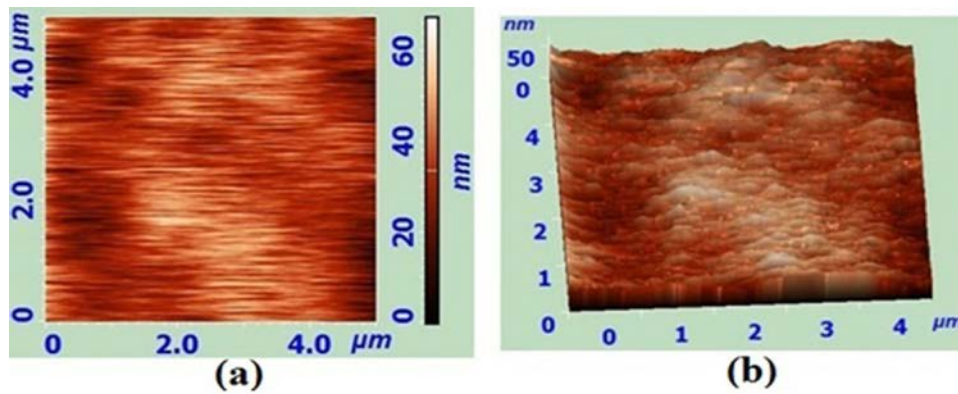


Fig. 2. AFM images of surface topography of Inconel 718 sample-7, (a) flattened corrected 2-dimensional image, (b) 3D image.

### 3.2. Discussion of Characterization of sample-14

Similar AFM examinations have also been performed on the sample-14 as on the sample-7 and relevant images have been acquired as explained in the previous subsection. Fig. 7 (a, b) demonstrated the 2-D micrographs and 3D topography of the surface of the sample-14. Figs. 8 (a, b & c) showed the cross section profiles of the surface along the horizontal line, vertical line, and slant line. The surface roughness profile and roughness pattern have been shown in Fig. (9). The threshold mask described the threshold at 33.52 nm and the numbers of grains are 212 at the scanned area of the surface of the sample-14 which is shown in Fig. (10). This image also revealed the grain structure and grain boundaries on the surface of the sample-14. The 2D and 3D FFT images of the sample surface after Fourier analysis have been shown in figure 11 (a, b). In Table 5, values of surface parameters of sample-14 have been presented.



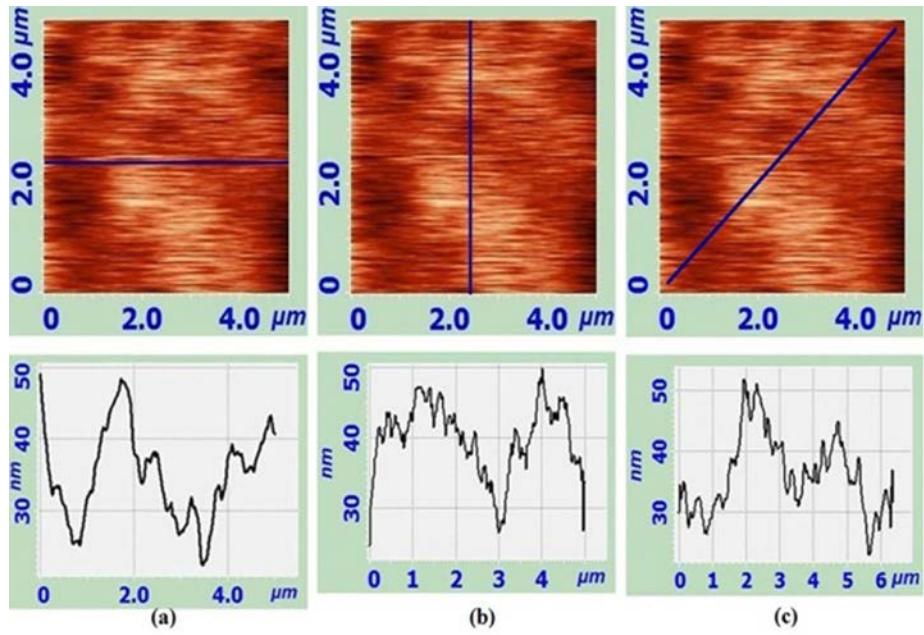


Fig. 3. Cross-section profiles of AFM images of sample-7 (a) X-axis line and related cross-section profile graph, (b) Y-axis line and related cross-section profile graph (c) slant line on and related cross-section profile graph.

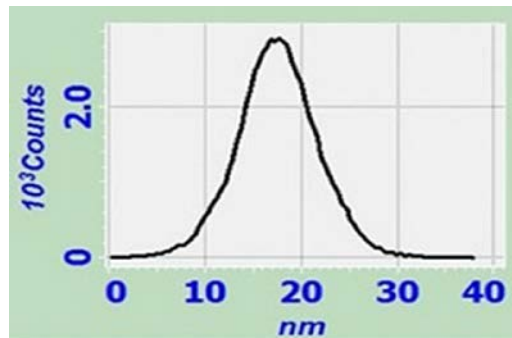


Fig. 4. Surface roughness analysis graph of sample-7.

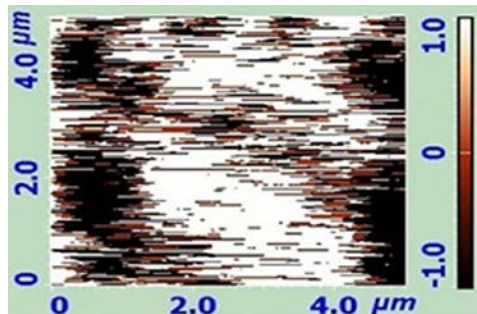


Fig. 5. AFM threshold mask image after grain analysis of sample-7.

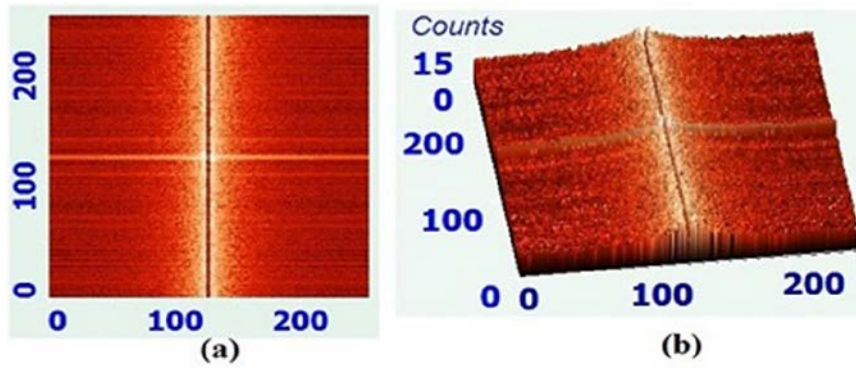


Fig. 6. AFM image of sample-7 after Fourier analysis using 2D FFT in logarithmic scaling, (a) 2-dimensional FFT image, (b) 3-dimensional FFT image.

Table 4

Surface parameters and related results obtained by AFM analysis of sample-7

| Sr. No. | Surface Parameter          | AFM Results |
|---------|----------------------------|-------------|
| 1       | Maximum height             | 37.74 nm    |
| 2       | Minimum height             | 0.00 nm     |
| 3       | Peak-to-peak, $S_y$        | 37.74 nm    |
| 4       | Ten point height, $S_z$    | 18.58 nm    |
| 5       | Average height             | 17.38 nm    |
| 6       | Average Roughness          | 4.15 nm     |
| 7       | Second moment              | 17.87       |
| 8       | Root Mean square, $S_q$    | 4.15 nm     |
| 9       | Surface skewness, $S_{sk}$ | 0.018       |
| 10      | Kurtosis                   | 0.336       |

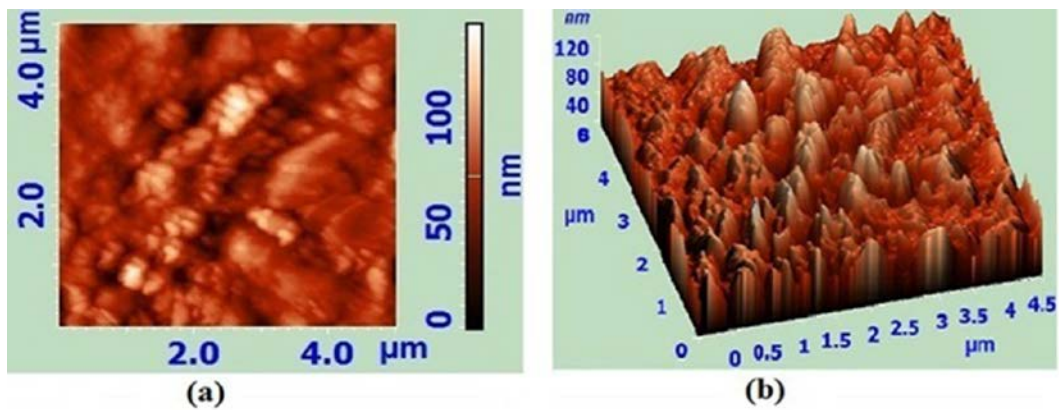


Fig. 7. AFM images of surface topography of Inconel 718 sample-14 (a) flatten corrected 2-dimensional image, (b) 3Dimensional image.

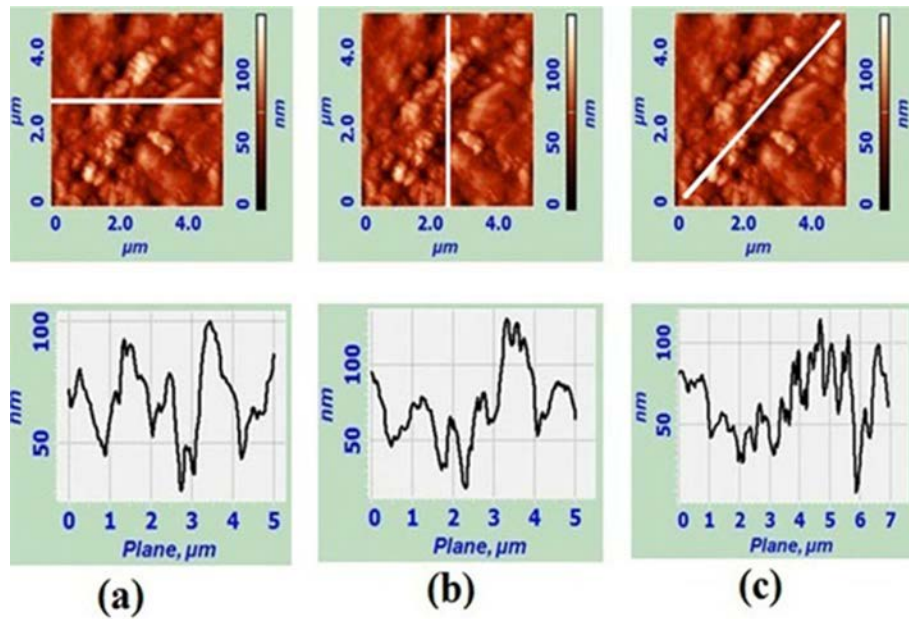


Fig. 8. Cross-section profiles of AFM images of sample-14 (a) X-axis line and related cross-section profile graph, (b) Y-axis line and related cross-section profile graph (c) slant line on and related cross-section profile graph.

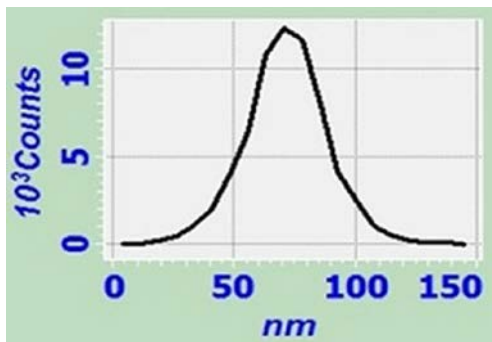


Fig. 9. Surface roughness analysis graph of sample-14.

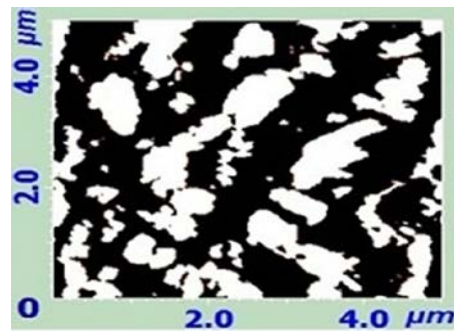


Fig. 10. AFM threshold mask image after grain analysis of sample-14

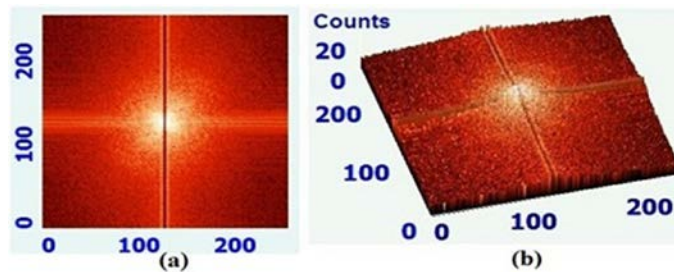


Fig. 11. AFM image of sample-14 after Fourier analysis using 2D FFT in logarithmic scaling, (a) 2-dimensional FFT image, (b) 3-dimensional FFT image.

Table 5

**Surface parameters and related results obtained by AFM analysis of sample-14.**

| Sr. No. | Surface Parameter          | AFM Results |
|---------|----------------------------|-------------|
| 1       | Maximum height             | 358.10 nm   |
| 2       | Minimum height             | 0 nm        |
| 3       | Peak-to-peak, $S_y$        | 358.10 nm   |
| 4       | Ten point height, $S_z$    | 181.88 nm   |
| 5       | Average height             | 171.31 nm   |
| 6       | Average Roughness          | 39.79 nm    |
| 7       | Second moment              | 178.14      |
| 8       | Root Mean square, $S_q$    | 48.85 nm    |
| 9       | Surface skewness, $S_{sk}$ | 0.065       |
| 10      | Kurtosis                   | -0.054      |

*3.3. Comparison of results of both the samples*

Table-4 and table-5 showed that different values of surface parameters have been acquired for both the samples such as average roughness value for sample-14 is 39.79 nm and that for sample-7 is 4.15 nm; root mean square value for sample-14 is 48.85 nm and that for sample-7 is 4.15 nm; surface skewness for sample-14 is 0.065 and that for sample-7 is 0.018, which are nearly same as Gaussian surface; and kurtosis for sample-14 is -0.054 and that for sample-7 is 0.336, which is less than the kurtosis of Gaussian surface. From these values of surface parameters and by observing all the AFM images from the Fig. 2 to Fig. 11, it has been revealed that sample-7, which is processed by using the second set of input parameters of wire EDM process, results in desirable and considerable surface characteristics rather than sample-14. It has been found that all the relevant images and values of surface parameters and topography are different to each other for both the samples. It has been summarized that surface preparation has the significant influence on the surface integrity of Inconel 718 sample machined by the different set of input parameters. Additionally, four numbers of confirmation tests have been accomplished using the cutting parameter setting of sample-7 & sample-14; and found the same results of surface roughness. The results acquired from confirmation experiments are reproducible.

**4. Conclusions**

In the present experimental research, Inconel 718 samples have been prepared by wire EDM process and probed their surface properties using stylus method as well as AFM technique. The surface parameters such as maximum height, ten point height, average roughness, skewness, second moment and kurtosis have been acquired by adopting AFM. The grain boundaries, grain structures and cross-section profiles and threshold of surfaces have been obtained

in micro and nano ranges. The surface integrity and topography of the samples of Inconel 718 material have also been evaluated and compared. In this study the following conclusions have been drawn:

1. The cutting conditions of the wire EDM process have significant effects on the surface integrity of samples.
2. Sample-7 exhibits the minimum surface roughness as compared to other samples, which indicates that the parameters setting used in preparing the sample-7 is the most optimum factor combination.
3. ANOVA results delineate that the cutting voltage is the most significant parameter, which has the greatest impact on the response parameter ( $R_a$ ) as the P-value of the parameter is 0.000.
4. It has been also reported from the ANOVA table that wire tension is the second important cutting factor as it possesses p-value of 0.002. Moreover, the cutting voltage and the wire tension are individually significant, their interaction is found insignificant.
5. The main effects plot for means of  $R_a$  has also illustrated that the cutting voltage is the most significant parameter as the inclined line is bigger than that of other parameters.
6. It can be summarized that the  $R_a$  value increases to  $3.25 \mu\text{m}$  when the pulse on time is raised to higher level and off time is reduced to lower level.
7. It has been also found that the  $R_a$  value is at minimum when the wire tension is increased to higher level and on time is at lower level.
8. As the cutting voltage and on time are reduced to minimum level, the surface roughness  $R_a$  obtained is also at minimum value.
9. When the wire tension is increased to higher level and off time is at lower level, there is significant decrease in the surface roughness  $R_a$ .
10. As the cutting voltage and off time are reduced to minimum level, the surface roughness  $R_a$  obtained is also at minimum value.
11. There is a significant increase in the surface roughness  $R_a$ , when cutting voltage is at higher level and wire tension is at minimum level.
12. AFM images imply that the surface topography and surface characteristics of machined sample-7 are excellent and splendid than those of other samples. Kurtosis value obtained for the surface of sample-7 is 0.336 which is less than the kurtosis of Gaussian surface, which signifies that the sample-7 is sound and congenial in terms of fine surface integrity.

#### REFERENCES

- [1] *K. J. Stout, L. Blunt*, Three-Dimensional Surface Topography, Penton Press, London, 2000.
- [2] *R. Leach*, Introduction to surface texture measurement, in: Leach, R. (Ed.), Optical Measurement of Surface Topography. Springer: Verlag Berlin Heidenberg, 2011, pp. 1-14.

- [3] D. J. Whitehouse, Handbook of Surface and Nanometrology, CRC press, Taylor & Francis Group, Boca Raton, FL, 2011.
- [4] U. Inan, C. Aydin, O. Uzun, O. Topuz, T. Alacam, Evaluation of the surface characteristics of used and new ProTaper instruments: an atomic force microscopy study. J. Endod., **vol. 33**, 2007, 1334-1337.
- [5] C. R. Valois, L. P. Silva, R. B. Azevedo, Atomic force microscopy study of stainless-steel and nickel-titanium files. J. Endod., **vol. 31**, 2005, pp. 882-885.
- [6] P. G. Ul'yanov, A. M. Dobrotvorskii, D. Y. Usachev, K. I. Borygina, V. K. Adamchuk, Atomic force microscopy of the nanostructure of metals and alloys subjected to mechanical and thermal stresses. Bull. Russ. Acad. Sci. Phys., **vol. 76**, 2012, pp. 149-152.
- [7] D. Kojić, L. Matija, L. Petrov, R. Mitrović, D. Koruga, Surface characterisation of  $Pb_{1-x}Mn_xTe$  alloy by atomic force microscopy and magnetic force mode. Surf. Eng., **vol. 27**, 2011, 158-163.
- [8] A. Thakur, S. Gangopadhyay, K. P. Maity, Effect of cutting speed and CVD multilayer coating on machinability of Inconel 825. Surf. Eng., **vol. 30**, 2014, pp. 516-523.
- [9] H. R. Tonday, and A. M. Tigga, Characterization of Surface Integrity of Ti6Al4V Alloy Machined by Using Wire Electrical Discharge Machining Process. Mater. Today: Proc., **vol. 11**, 2019, A8-A14.
- [10] Z. C. Lin, Y. C. Hsu, A study of estimating cutting depth for multi-pass nanoscale cutting by using atomic force microscopy. Appl. Surf. Sci., **vol. 258**, 2012, pp. 4513-4522.
- [11] M. Imran, P. T. Mativenga, A. Gholinia, P. J. Withers, Evaluation of surface integrity in micro drilling process for nickel-based superalloy. Int. J. Adv. Manuf. Technol., **vol. 55**, 2011, 465-476.
- [12] S. A. Krishnan, G. L. Samuel, Multi-objective optimization of material removal rate and surface roughness in wire electrical discharge turning. Int. J. Adv. Manuf. Technol., **vol. 67**, 2013, 2021-2032.
- [13] M. Ay, U. Çaydaş, A. Hasçalık, Optimization of micro-EDM drilling of Inconel 718 superalloy. Int. J. Adv. Manuf. Technol., **vol. 66**, 2013, 1015-1023.
- [14] K. Kanlayasiri, and S. Boonmung, Effects of wire-EDM machining variables on surface roughness of newly developed DC 53 die steel: Design of experiments and regression model. J. Mater. Process. Technol., **vol. 192**, 2007, 459-464.
- [15] T. A. Spedding, Z. Q. Wang, Parametric optimization and surface characterization of wire electrical discharge machining process. Precis. Eng., **vol. 20**, 1997, pp. 5-15.
- [16] A. A. Fedorov, A. I. Blesman, D. V. Postnikov, D. A. Polonyankin, G. S. Russkikh, & A. V. Linovsky, Investigation of the impact of Rehbinder effect, electrical erosion and wire tension on wire breakages during WEDM. J. Mater. Process. Technol., **vol. 256**, 2018, 131-144.
- [17] A. M. Takale, & N. K. Chougule, Effect of wire electro discharge machining process parameters on surface integrity of Ti49. 4Ni50. 6 shape memory alloy for orthopedic implant application. Mater. Sci. Eng. C, **vol. 97**, 2019, 264-274.
- [18] H. R. Tonday, and A. M. Tigga, An empirical evaluation and optimization of performance parameters of wire electrical discharge machining in cutting of Inconel 718. Meas., **vol. 140**, 2019, 185-196.